Supporting Information

Porous $ZrNb_{24}O_{62}$ Nanowires with Pseudocapacitive Behavior Achieve High-Performance Lithium-Ion Storage

Chao Yang,[1,2] Yelong Zhang,[2] Fan Lv,[2] Chunfu Lin,[1]* Yao Liu,[5] Kai Wang,[2] Jianrui Feng,[2] Xiaohong Wang,[1] Yongjun Chen,[1] Jianbao Li,[1] and Shaojun Guo[2,3,4]*

[1]State Key Laboratory of Marine Resource Utilization in South China Sea, College of Materials and Chemical Engineering, Hainan University, Haikou 570228, Hainan, China.

[2]Department of Materials Science and Engineering, College of Engineering, Peking University, Beijing 100871, China.

[3]BIC-ESAT, College of Engineering, Peking University, Beijing 100871, China.

[4]Key Lab of Theory and Technology for Advanced Battery Materials, College of Engineering, Peking University, Beijing 100871, China.

[5]Department of Chemistry and Shanghai Key Laboratory of Molecular Catalysis and Innovative Materials, Institute of New Energy, Fudan University, Shanghai 200433, China.

Email: linchunfu@hainu.edu.cn; guosj@pku.edu.cn

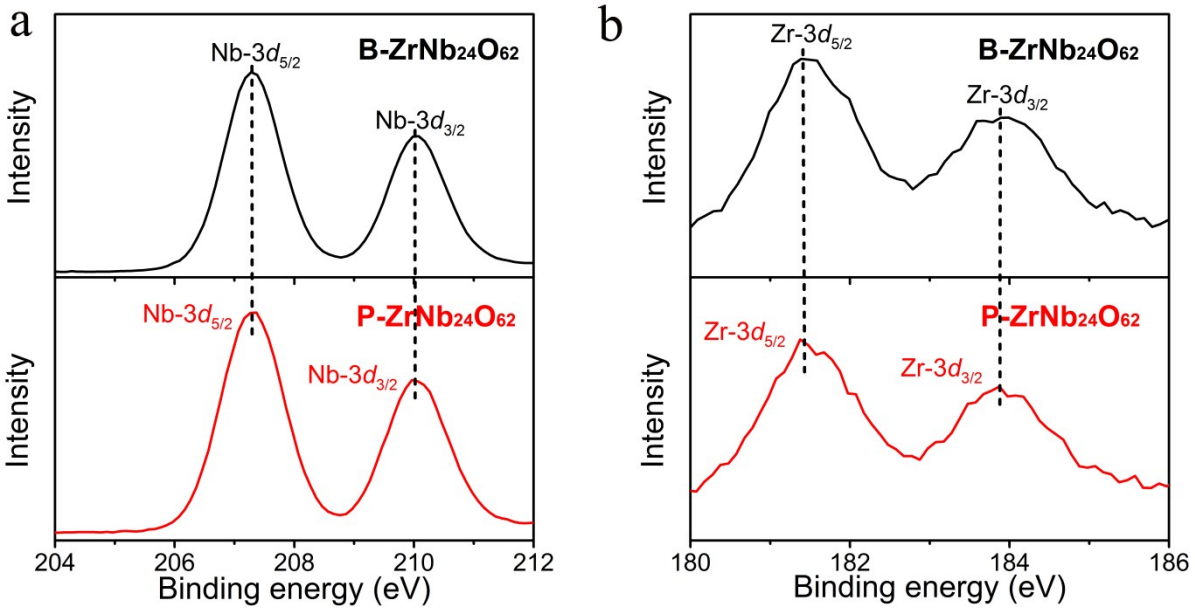

Fig. S1 XPS spectra of (a) Nb and (b) Zr in B-$ZrNb_{24}O_{62}$ and P-$ZrNb_{24}O_{62}$.

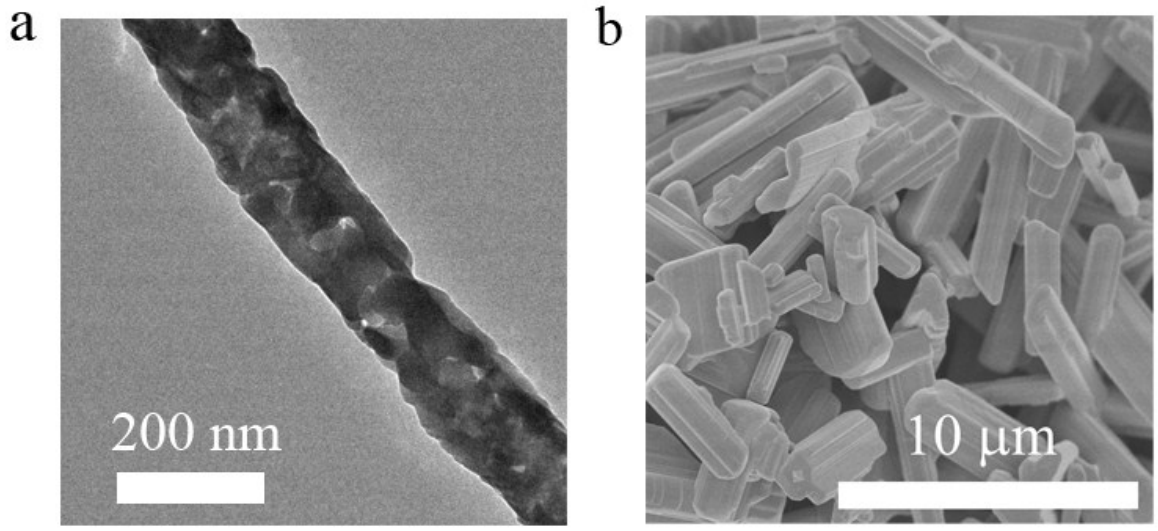

Fig. S2 (a) High magnification TEM image of P-$ZrNb_{24}O_{62}$; (b) SEM image of B-$ZrNb_{24}O_{62}$ with an average size of ~1.6 μm.

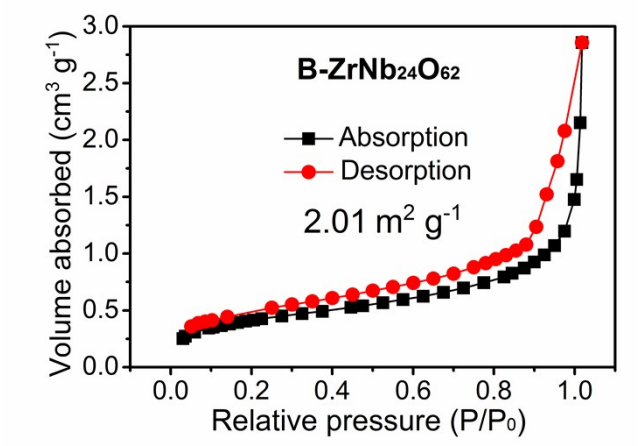

Fig. S3 N_2 adsorption–desorption isotherm of B-$ZrNb_{24}O_{62}$.

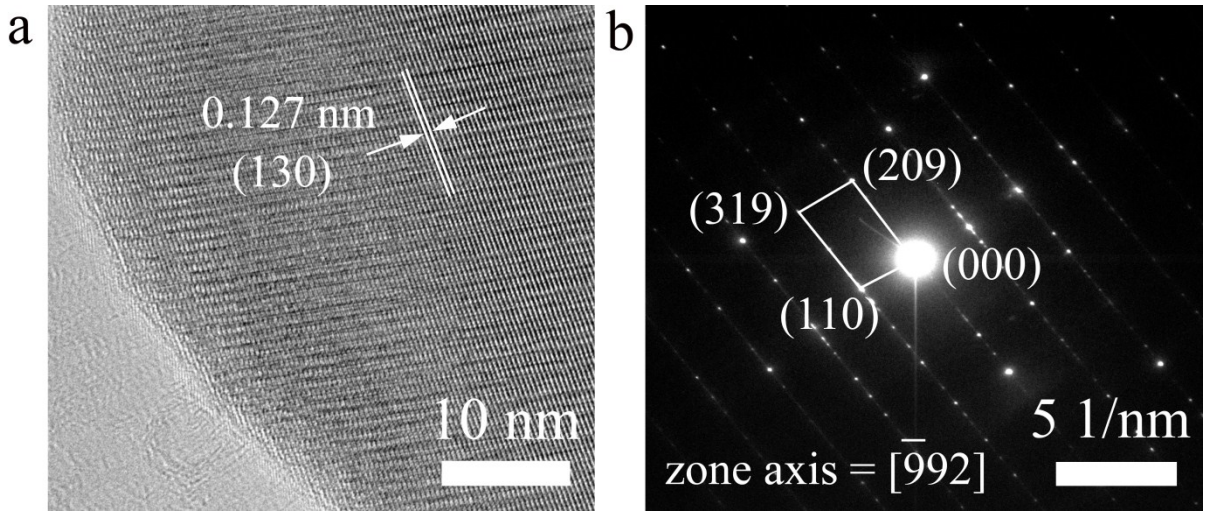

Fig. S4 (a) HRTEM image and (b) SAED pattern of B-$ZrNb_{24}O_{62}$.

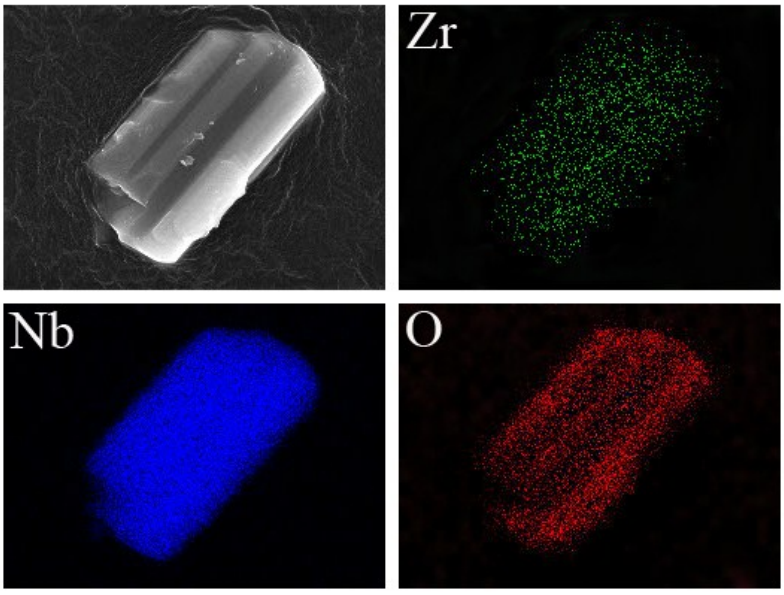

Fig. S5 EDX mapping image of B-$ZrNb_{24}O_{62}$.

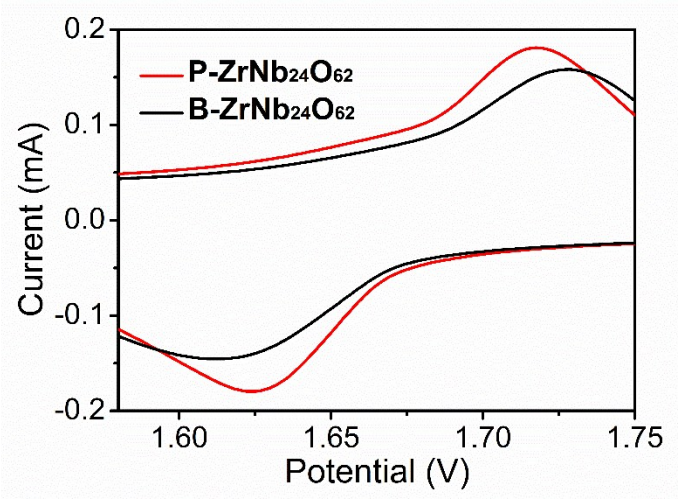

Fig. S6 CV curves of B-$ZrNb_{24}O_{62}$/Li and P-$ZrNb_{24}O_{62}$/Li cells between 1.58 V and 1.75 V at 0.1 mV s^{-1} (2^{nd} cycle).

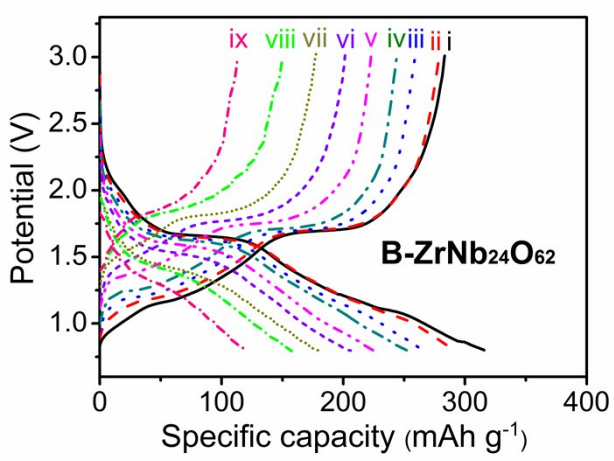

Fig. S7 (i) First-cycle discharge–charge curves of B-$ZrNb_{24}O_{62}$/Li cell at 0.1 C and second-cycle discharge–charge curves at (ii) 0.1, (iii) 0.5, (iv) 1, (v) 2, (vi) 5, (vii) 10, (viii) 20 and (ix) 30 C.

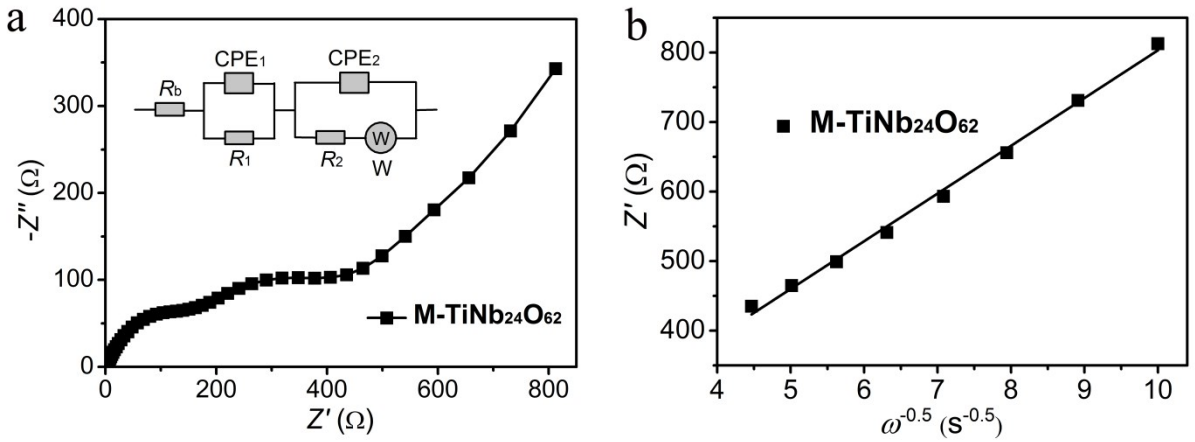

Fig. S8 (a) Nyquist plot of M-$TiNb_{24}O_{62}$/Li cell (M-$TiNb_{24}O_{62}$: micron-sized $TiNb_{24}O_{62}$ particles, *inset*: selected equivalent circuit). (b) Relationship between real impedance with low frequency for M-$TiNb_{24}O_{62}$/Li cell. The obtained R_b, R_1, R_2, σ and D values are 2.61 Ω, 209 Ω, 677 Ω, 66.7 Ω $s^{-0.5}$ and 2.13 × 10^{-14} cm^2 s^{-1}, respectively.

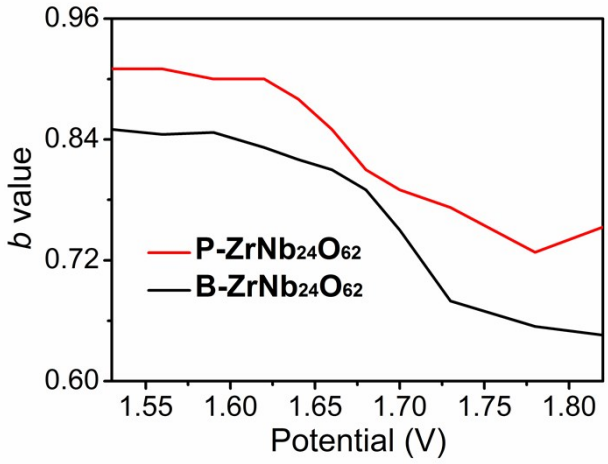

Fig. S9 Determination of the anodic *b*-values at different potentials during delithiation for B-$ZrNb_{24}O_{62}$/Li and P-$ZrNb_{24}O_{62}$/Li cells.

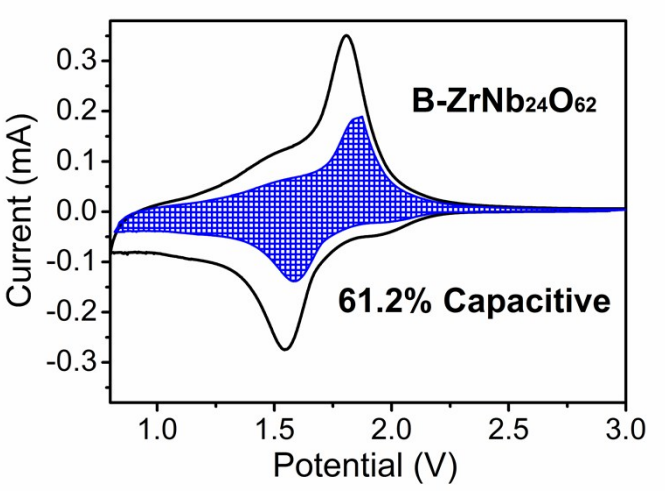

Fig. S10 CV curve of B-$ZrNb_{24}O_{62}$/Li cell with pseudocapacitive fraction (blue region) at 1.1 mV s^{-1}.

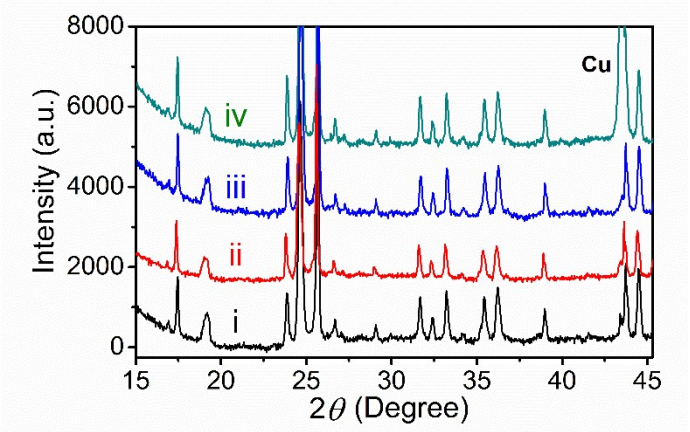

Fig. S11 *Ex-situ* XRD patterns of B-$ZrNb_{24}O_{62}$ electrodes after (i) as-fabricated, (ii) discharged to 0.8 V in 1st cycle, and charged to 3.0 V in (iii) 1st and (iv) 100th cycles at 0.1 C.

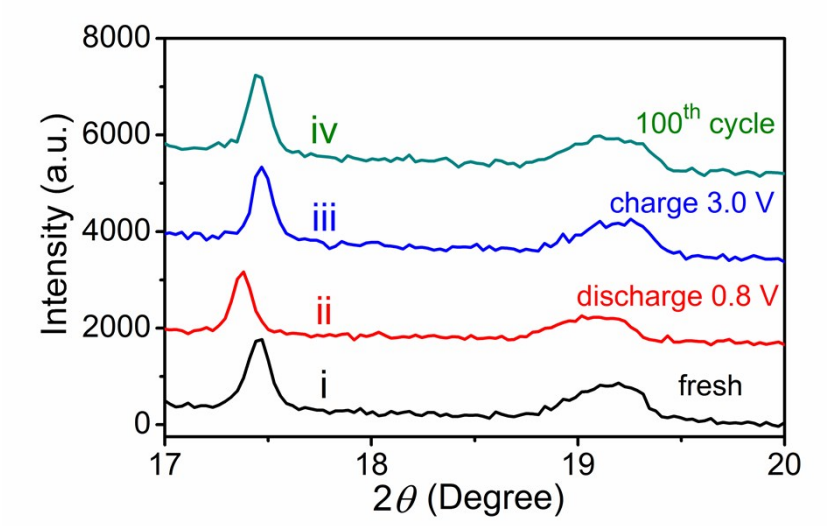

Fig. S12 *Ex-situ* XRD patterns of B-$ZrNb_{24}O_{62}$ electrodes after (i) as-fabricated, (ii) discharged to 0.8 V in 1st cycle, and charged to 3.0 V in (iii) 1st and (iv) 100th cycles at 0.1 C in 17.0º–20.0º.

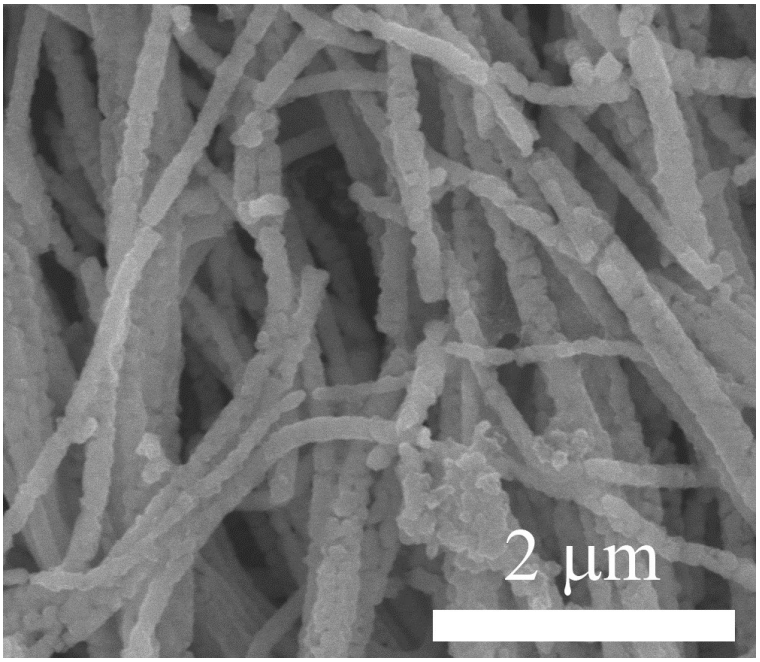

Fig. S13 *Ex-situ* SEM image of P-$ZrNb_{24}O_{62}$ electrode after 1500 cycles at 10 C.

Table S1 Results of crystal analyses by Rietveld refinements in $ZrNb_{24}O_{62}$ and $TiNb_{24}O_{62}$.

Sample	Space group	a (Å)	b (Å)	c (Å)	α, γ (°)	β (°)	V (Å^3)	R_{wp}*	Reference
$ZrNb_{24}O_{62}$	$C2$	29.8712 3(255)	3.8220 9(26)	21.1637 9(157)	90	95.07 8(7)	2406.79 8(430)	0.1146	this work
$TiNb_{24}O_{62}$	$C2$	29.7921 2(173)	3.8175 1(20)	21.0998 6(114)	90	95.01 8(5)	2390.52 6(288)	0.1067	[S1]

* Weighted profile residual.

Table S2 Fractional atomic parameters of $ZrNb_{24}O_{62}$ with *C2* space group. During the refinement, the following instrumental/structural parameters were successively refined: background parameters, zero-shift, lattice parameters, profile parameters, atomic fractional coordinates and atomic isotropic temperature factors. The site occupancies of Zr^{4+}, Nb^{5+} and O^{2-} ions were fixed to be 0.04, 0.96 and 1, respectively. All the isotropic temperature factors were fixed to be the same.

Atom*	Symmetry	Site	*x*	*y*	*z*
M1	2	2a	0	0.25	0
M2	1	4c	0.1140	0	0.0123
M3	1	4c	0.2449	0	0.0552
M4	1	4c	0.3706	0	0.1148
M5	1	4c	0.4972	0	0.1629
M6	1	4c	0.0915	0	0.1782
M7	1	4c	0.2174	0	0.2361
M8	1	4c	0.3451	0	0.2869
M9	1	4c	0.4783	0	0.3320
M10	1	4c	0.0707	0	0.3598
M11	1	4c	0.1965	0	0.4151
M12	1	4c	0.3220	0	0.4614
M13	1	4c	0.4452	0	0.5125
O1	1	4c	0.3852	0	0.0166
O2	1	4c	0.1770	0	0.0308
O3	1	4c	0.3081	0	0.0934
O4	1	4c	0.1026	0	0.1025
O5	1	4c	0.4371	0	0.1384
O6	1	4c	0.2285	0	0.1510
O7	1	4c	0.0017	0	0.1506
O8	1	4c	0.3563	0	0.2013
O9	1	4c	0.1475	0	0.2118
O10	1	4c	0.4936	0	0.2465
O11	1	4c	0.2858	0	0.2581

O12	1	4c	0.0737	0	0.2718
O13	1	4c	0.4243	0	0.3098
O14	1	4c	0.2015	0	0.3254
O15	1	4c	0.3381	0	0.3823
O16	1	4c	0.1287	0	0.3914
O17	1	4c	0.4663	0	0.4429
O18	1	4c	0.2500	0	0.4360
O19	1	4c	0.0429	0	0.4695
O20	1	4c	0.3929	0	0.4954
O21	1	4c	0.1814	0	0.5229
O22	1	4c	0.3113	0	0.5721
O23	1	4c	0.4402	0	0.6184
O24	1	4c	0.0221	0	0.6663
O25	1	4c	0.1527	0	0.7190
O26	1	4c	0.2811	0	0.7553
O27	1	4c	0.4166	0	0.8512
O28	1	4c	0.1238	0	0.9148
O29	1	4c	0.4723	0	0.9156
O30	1	4c	0.2470	0	0.9567
O31	1	4c	0.0376	0	0.9696

* M = 0.04Zr + 0.96Nb

Table S3 Potentials at intensive cathodic/anodic CV peaks and potential differences of B-$ZrNb_{24}O_{62}$/Li and P-$ZrNb_{24}O_{62}$/Li cells at 0.1 mV s^{-1} (2^{nd} cycle).

Sample	Potential at intensive cathodic peak (V)	Potential at intensive anodic peak (V)	Potential difference (V)
B-$ZrNb_{24}O_{62}$	1.610	1.731	0.121
P-$ZrNb_{24}O_{62}$	1.626	1.717	0.091

Table S4 Impedance parameters and Li^+-ion diffusion coefficients of B-$ZrNb_{24}O_{62}$ and P-$ZrNb_{24}O_{62}$.

Sample	R_b (Ω)	R_1 (Ω)	R_2 (Ω)	σ (Ω $s^{-0.5}$)	D (cm^2 s^{-1})
B-$ZrNb_{24}O_{62}$	2.19	196	621	61.3	3.76×10^{-14}
P-$ZrNb_{24}O_{62}$	2.36	87	205	7.43	2.47×10^{-13}

Reference

[S1] C. Yang, S. J. Deng, C. F. Lin, S. W. Lin, Y. J. Chen, J. B. Li, H. Wu, *Nanoscale,* 2016, **8**, 18792.